Lab On Skin™: 3D Monolitically Integrated Zero-Energy Micro/Nanofludics and FD SOI Ion Sensitive FETs for Wearable Multi-Sensing Sweat Applications

F. Bellando[1], E. Garcia-Cordero[1], F. Wildhaber[2], J. Longo[2], H. Guérin[2,1] and A.M. Ionescu[1]
[1]Nanolab, Ecole Polytechnique Fédérale de Lausanne, Switzerland, email: {francesco.bellando@epfl.ch, adrian.ionescu@epfl.ch}
[2]Xsensio S.A., EPFL Innovation Park, 1024 Ecublens, Switzerand {hoel.guerin@xsensio.com, hoel.guerin@epfl.ch}

***Abstract*—** This paper reports a novel fully integrated low power multi-sensing smart system, which, by wafer-level 3D heterogeneous integration of Ion Sensitive Fully Depleted (FD) FETs and SU-8 micro/nanofludics, achieves the first of its kind wearable multi-sensing system, called Lab on Skin™, capable to detect biomarkers in human sweat. In the reported configuration, the multi-sensing system exploits arrays of functionalized sensors capable to simultaneously detect pH, Na^+ and K^+ concentrations in sweat in real time. We present a detailed electrical DC and dynamic characterization, showing excellent sensitivities (52mV/dec for pH and -37mV/dec for Na^+ sensors) with ultra-low power consumption (less than 50 nWatts/sensor). We report ion cross-sensitivities and a differential measurement approach that allows calibrated measurements. Overall, the paper reports significant advances in the design and fabrication of micro/nanofludics channels, inlets compatible with human skin pore size and density, and outlet passive pumps with flow rates of tens of pl/s; all capable of exploiting capillary forces in order to provide a zero energy pumping of sweat into sensing channels. Moreover, we report the first integration of a miniaturized Ag/AgCl Quasi-Reference Electrodes (QRE) into the sensing system, with long term stability, paving the way for fully wearable electronic chips in flexible patches or as plug-in modules in wrist based devices.

I. Introduction and Rationale

Wearable biosensors [1-2] hold promise for playing a significant role in future personalized and preventive healthcare as they enable non-invasive and real time monitoring of a large variety of biomarkers in human biofluids. They add significant value to activity monitoring, which is tracked by MEMS sensor technology (accelerometers and gyroscopes), and, to other biosignals (such as heart rate and blood oxygenation). Moreover, sweat is easily accessible via the largest human organ, the skin, and can take advantage of patch and wrist-based device embodiments. Previous reports on the detection of biomarkers in sweat were based on large electrochemical sensors [3-4] requiring large amounts of sweat, which limits the field of applications to sport with abundant sweating or requires pilocarpine-induced cholinergic sweating, which is not user friendly and can even modify the physiological composition of sweat.

A recent comprehensive review [5] reported that there are hundreds of biomarkers that can be tracked in human sweat and, for some, the correlations with the concentrations of same type of biomarkers in blood, considered as the gold standard, are fully demonstrated. Among detectable sweat markers, the ions or electrolytes with mM concentrations such as Na^+, K^+, H^+, NH_4^+, Ca^{2+}, Cl^-, form a family of high interest for a large variety of applications, ranging from complex body states such as hydration, to heart and metabolic diseases. Other biomarkers such as glucose, lactate, uric acid and ethanol are detectable in sweat. Recent reports showed the detection of lactate monitoring with conventional components on a wireless potentiostat board [6], the integration of graphene-based glucose/oxygen enzymatic fuel cell into a band-aid patch for detecting glucose in sweat [7], and, the monitoring of alcohol lifestyle through the detection of ethylglucuronide (EtG), a metabolite of ethanol [8].

Therefore, sweat is a very attractive biofluid for personalized and preventive healthcare that needs to fulfill wearability requirements. These requirements concern *robust* multisensing in *small form factor*, with both *high selectivity* and *high sensitivity*, *low power consumption*, *bio-compatibility* and *capability of collecting sweat in situ* and measure it in real time. Recently, we have reported the advantages of customizing FinFET CMOS technology to co-integrate sensing functions, as a step forwards to low power robust wearable biosensing [9, 10].

In this paper, we present for the first time a fully compact smart multi-sensing technology capable of: (i) multi-ion detection using arrays of FD SOI FETs with liquid gates, specifically functionalized for certain classes of electrolytes, (ii) the wafer-level integration of double-layer SU-8 passive, micro/nanofludic channels on SOI FETs, capable to collect and conduct the sweat to the FET sensors by the use of microcapillary forces, resulting in zero energy sweat pumping, and, (iii) the integration at the first level of metal interconnects of a miniaturized Ag/AgCl electrode capable to offer stable and fully calibrated measurements of biomarkers in sweat. The concept results in micro/nano-fludics/nano-electronic chips that can be functionalized to a large number of biomarkers and form the first of its kind Lab On Skin™ technology platform.

II. Lab On Skin: Concept, Design, Fabrication

The Lab On Skin concept is depicted in the 3D embodiment showed in Fig. 1. The reported design includes four different sensor arrays based on ionic-sensitive FD SOI sensors with high-k dielectric gate stack: (1) bare HfO_2 gate stack sensors array for pH sensing, (2) a non-functionalized gold/HfO_2 sensor array serving as control (reference) device

and (3) functionalized gold/HfO_2 gate stacks arrays with specific crown molecules for Na^+ and K^+ detection.

FABRICATION PROCESS: FD SOI ISFET WITH WAFER-LEVEL 3D INTEGRATED SU-8 MICRO/NANOFLUDICS

The main fabrications steps of the Lab On Skin are described in Fig. 2. The devices are built on Fully-Depleted (FD) SOI substrate, which allows excellent electrostatic control and low leakage current. The SOI FET sensors have ribbon-like form factors, with a Si film thickness of 30 nm and channel widths ranging from 0.8 to 4 µm. The 3 nm HfO_2 gate dielectric offers nearly ideal Nernstian sensitivity to pH and ultra-low gate leakage. The ALD deposition of HfO_2 is performed on top of 2 nm of dry thermal SiO_2 resulting in a low defect interface. AlSi 1% metal lines are deposited by lift-off. The pH sensors have no metallization on the high-k gate stack (sensor #1). 100 nm layer of gold is sputtered on top of the dielectric for the ion sensors (the control sensor#2 and the functionalized-on-gold Na^+ sensor#3 and the K^+ sensor#4) that need functionalization and for the control sensors. Next, a 3 µm layer of SU-8 photoepoxy is processed on top of the wafer to isolate FET sensor interconnects, with openings left only in the sensor channel regions, contact pads and QRE. Next, the wafer is passivated with a photoresist, exposing the gold layer pattern for the creation of the RE. A 3 µm layer of silver (Ag) is electroplated on top of the exposed gold and is chlorinated to obtain a miniaturized QRE with a 3.6 µm thickness (Fig. 4).

The wafer-level 3D integration of micro/nanofluidic channels is summarized in Fig. 2. A biocompatible 30µm layer of SU-8 is processed on top of the SOI wafer with passivated FET sensors (wafer#1). This layer corresponds to the channels and micropumps of our microfluidic layer. In order to close the channels, a second SU-8 wafer is processed. A 500 nm layer of Al is sputtered, followed by a 30 µm layer of SU-8. Afterwards, the wafers are put in contact while applying 120°C and 4 bars. This step allows the bonding of SU-8 layers. The wafers are placed in a 1M NaCl solution and a 5V potential is applied to achieve anodic dissolution of Al, which releases the top wafer. Finally, arrays of inlets with 90 µm diameters are drilled with an excimer laser.

ZERO-ENERGY SUB-NANO-LITER PUMPING TECHNOLOGY WITH EMBEDDED QUASI-REFERENCE ELECTRODE

In order to achieve ultra-low energy consumption, a capillary driven microfluidics has been designed. The design accounts for the density of skin pores, the average sweat rate of humans (≈ 5 nL/min) and the need of constant flow rate at sensor level. To achieve this, a capillary pump was added in the channel (Figs. 1 and 3). SU-8 is the microfluidic material of choice due to its compatibility with microtechnology, robustness, biocompatibility and contact angle (64.1°), which activates the capillary driven sub-nano-liter flow. We have validated one of the first autonomous capillary system capable of keeping a constant flow rate for extremely low volumes of liquid. The proposed micro pump provides a constant unidirectional flow of only 120 pL/minute (Fig. 3a). This low rate ensures channel and QRE wetting (Fig. 3b) while the sweat analysis is performed in seconds/minutes.

We report fully integrated RE (Fig. 4), co-integrated with microfluidics and sensors; a Chlorination process produces the stable Ag/AgCl micrometer size QREs.

FD SOI FET SENSOR FUNCTIONALIZATON

The functionalization of the FET is based on a thiol-gold interaction between thiolated ion-sensitive crown ethers and the gold gate of the sensor. The first part of the process is dedicated to the hydroxy to thiol crown ether modification, Fig. 5 (a). The alcohol group of the crown ether is converted to a sulfonate (leaving group) using toluenesulfonyl chloride. A nucleophilic substitution using 2,2'.(ethylenedioxy)-diethanedithiol is performed to obtain a thiol functionalized crown ether. The FET arrays are functionalized for K^+ and Na^+ sensing (Fig. 5 (b) and (c)) by putting them 12 hours in contact with a solution of thiolated crown-ethers in methanol.

III. ELECTRICAL CHARACTERIZATION AND DISCUSSION

Figs. 6 and 7 report the characterization of the pH sensor#1 with HfO_2 gate; a full scale sensitivity of 52.8mV/pH is extracted in weak inversion, at constant current of 40 nA. The inset of Fig. 6 shows a metal gate FD SOI FET that has a quasi-ideal subthreshold swing, SS, of 62mV/dec and ultra-low I_{off} current. The dynamic ISFET response is in Fig. 8, showing excellent stability and a time response lower than 5s. Figs. 9, 10 and 11 show the characterization of selective sensing of the functionalized Na^+ devices (sensor#3) by observing a differential response to the concentration of Na^+ with respect to the control sensor#2, for concentrations of ions similar to the ones in sweat; a value of -37mV/dec differential sensitivity is found. Fig. 12 shows the dynamic measurement of same differential sensitivity to Na^+. Fig. 13 and 14 reports sets of I_D-V_G cross-sensitivity plots of control and Na^+ sensors to pH (needed for simultaneous multi-sensing). Fig. 15 demonstrates that no significant difference is observed when testing ion concentration with different pH. Fig. 16 reports the response to K^+ ions of the control sensor, needed for similar differential measurements. Finally, in Fig. 17 we report the results of our integrated Ag/AgCl QRE; after coating with polyvinyl butyral/NaCl matrix [3], the integrated Ag/AgCl RE is fully stable, ensuring long term stable operation (days to weeks).

IV. CONCLUSIONS

We have reported the design, fabrication and experimental validation of a multi-sensing micro/nanosystem platform, Lab On Skin, capable to both collect passively (zero-energy microfluidcs) a biofluid and measure its biomarker content, in real time and with low energy; this is expected to enable future biosensing wearables for lifestyle and precision healthcare.

ACKNOWLEDGMENT

The authors acknowledge funding from ERC Advanced Grant Millitech and Swiss National Science Foundation via Flag-Era CONVERGENCE project.

REFERENCES

[1] D.H. Kim et al, Science, 333, 2011, pp. 838-43.
[2] W-Gao et al, IEDM 2016, pp. 161-164.
[3] W. Gao et al., Nature 529, 2016, 509–514.
[4] D. P. Rose et al, IEEE Trans on Biomed. Eng., 2015, pp. 1457-1465.
[5] J. Heikenfeld, Electroanalysis, 28, 2016, pp. 1-9.
[6] J. Dieffenderfer et al, IEEE Sensors, 2016.
[7] E. Cho etal, IEEE MEMS Conf. 2017, pp.366-369.
[8] D. Kinnamon et al, IEEE Sensors, 2016, pp. 1 -3.
[9] S. Rigante et al., ACS Nano, 2015, 9 (5), pp 4872–4881.
[10] E. Garcia-Cordero et al., ESSDERC/ESSCIRC 2016, pp. 452-455.
[11] C. Vericat et al., RSC Advances. vol.4. 2014, pp.27730-27754.

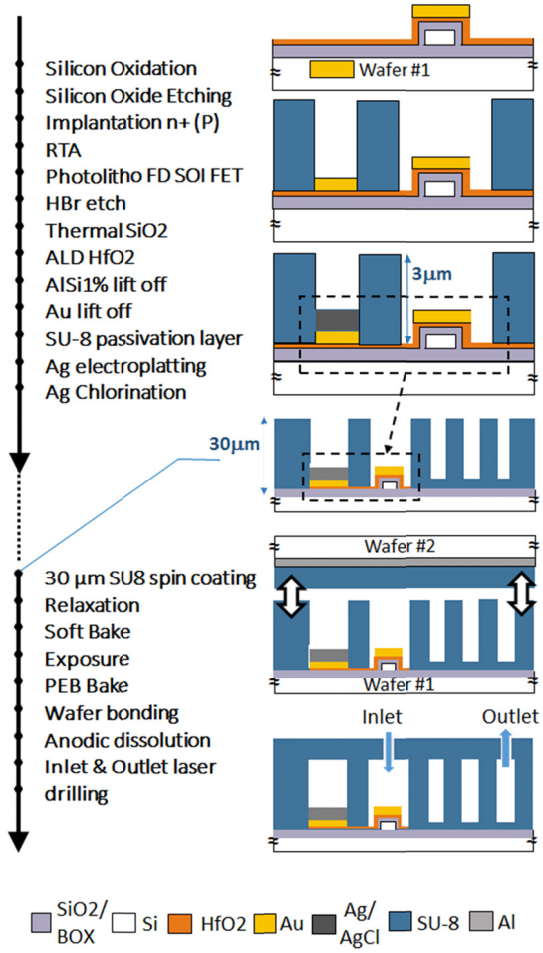

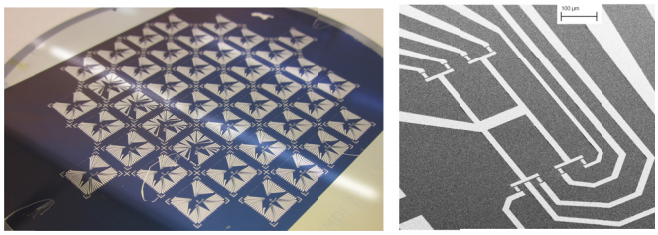

Fig. 2. *Top:* Wafer level fabrication process for Lab on Skin™ sensing microsystems including high-k metal gate SOI FD ISFET sensors, passivation, integration of Ag/AgCl Quasi-Reference Electrode (Wafer#1) and 3D heterogeneous integration of SU-8 microfluidics for sweat collection (Wafer#2), all in chip size of 9x9 mm, processed on 4 inches wafers. *Bottom:* top view of Wafer #1 and SEM zoom on a fabricated FD SOI ISFET sensor array of 8 sensors.

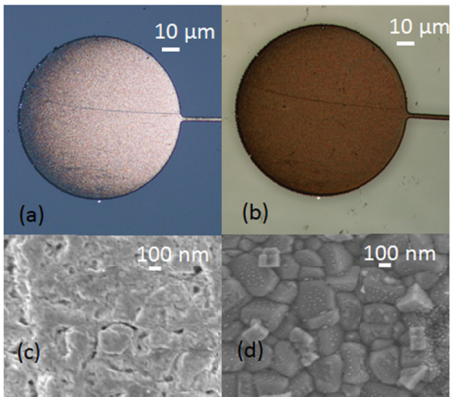

Fig. 4. Top optical views, (a) and (b), and SEM magnifications, (c) and (d), of the fabricated Ag/AgCl Quasi-Reference Electrode (QRE), before and after the Chlorination.

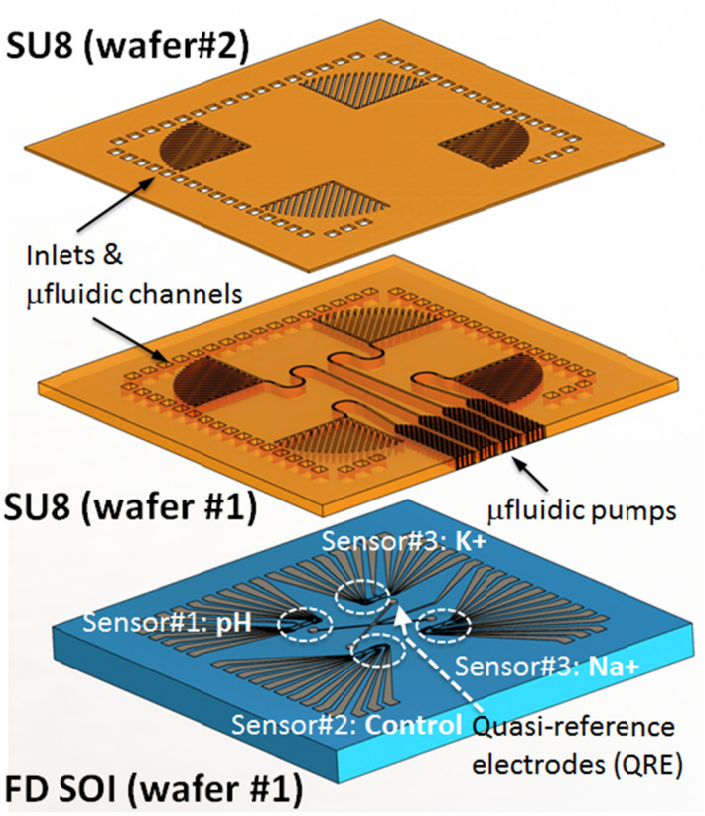

Fig. 1. *Top:* Lab On Skin™ concept, depicting the design of the sensing and microfluidics layers, with a 3D perspective the various layers. *Bottom:* Wafer level view, after FD SOI ISFET and first layer of SU-8 passivation.

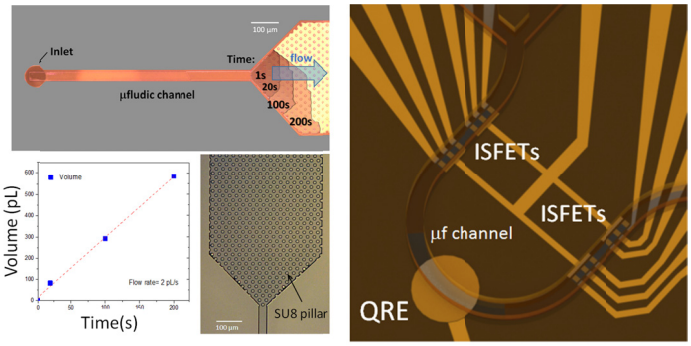

(a) (b)

Fig. 3. (a) *Top:* Design and operation (propagation of a biofluid with similar ionic concentration to sweat) of zero-energy microfluidic pumps exploiting microcapillary forces. *Bottom:* Experimental data showing a pump flux rate of 2 pico liter /second and zoom on constituent SU-8 micro-pillars. (b) Pseudo-color zoom on a microfluidic channel over Au gate ISFET and QRE.

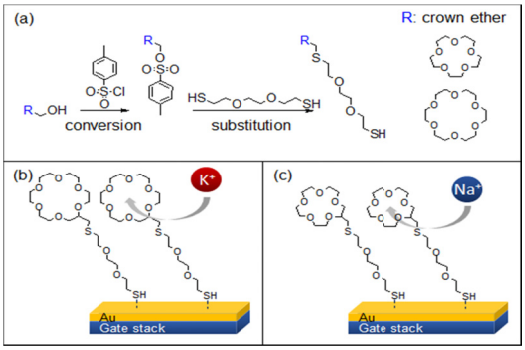

Fig. 5. Functionalization chemistry of the Au gates for specific electrolyte sensors: (a) hydroxy crown ethers modification, (b) and (c) FET gold gate functionalization for K^+ and Na^+ sensing, respectively.

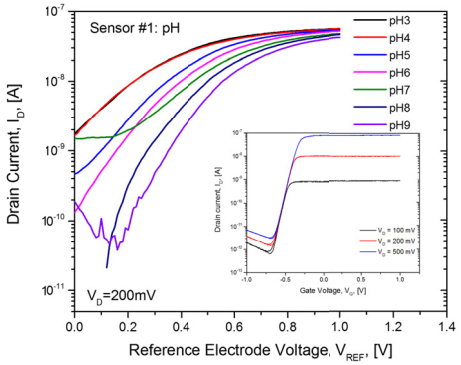

Fig. 6. I_DV_G characteristics of the pH sensor with HfO_2 gate for various pH buffers. Inset: FD SOI FET with metal gate and near ideal 62mV/dec swing.

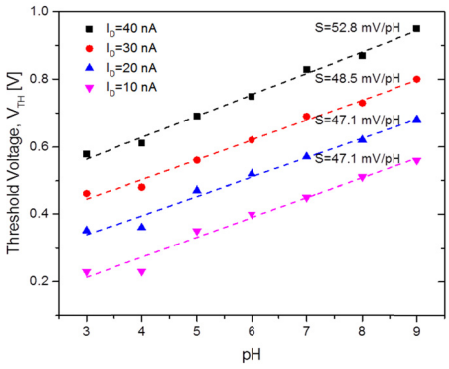

Fig. 7. pH sensitivities extracted at different drain current levels from data of Fig. 6.

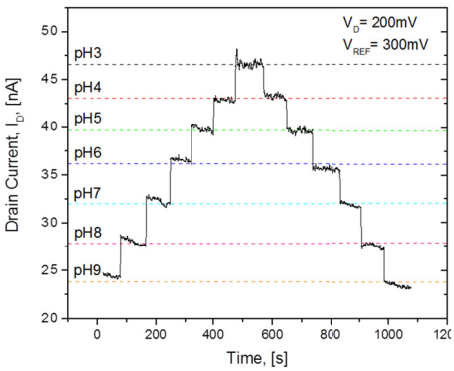

Fig. 8. Full-scale dynamic measurement of pH showing FD SOI ISFET time response < 5s.

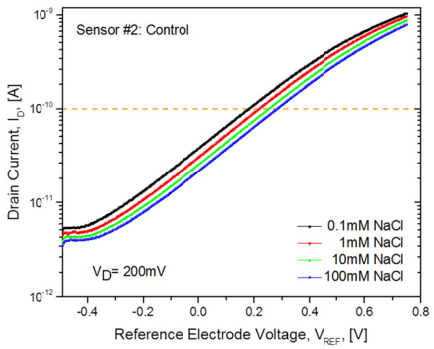

Fig. 9. I_D-V_G characteristics of the control sensor#2 (non-functionalized gold gate) for various molar concentrations of NaCl.

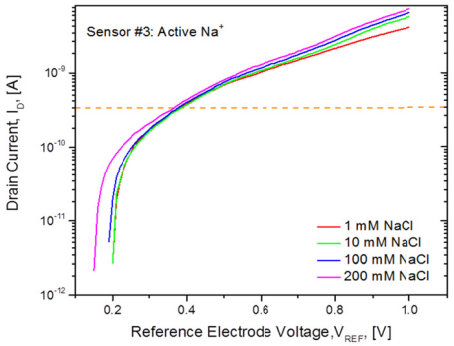

Fig. 10. I_D-V_G characteristics of the Na^+ sensor#3 (gold gate functionalized for Na^+) for various molar concentrations NaCl.

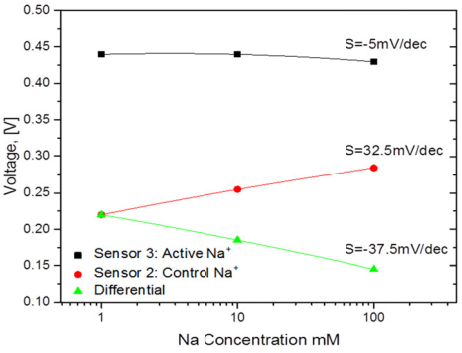

Fig. 11. Na^+ sensitivities of Na^+ sensor#3 and control sensor#2 and extraction of the differential *selective* sensitivity ($S_{D[Na+]}$=-37.5mV/dec).

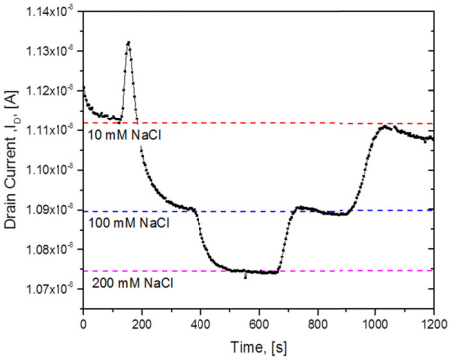

Fig. 12. Dynamic measurement of the Na^+ differential sensitivity (using differential measurement between sensors #2 and #3).

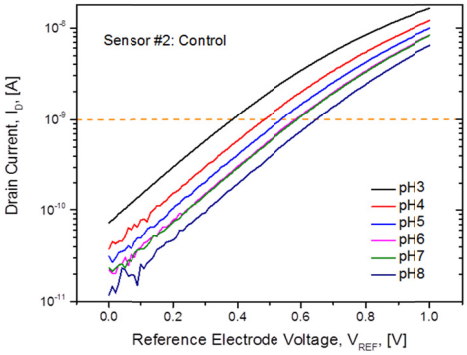

Fig. 13. I_D-V_G characteristics of the control sensor#2 (non-functionalized gold gate) for various pH buffers.

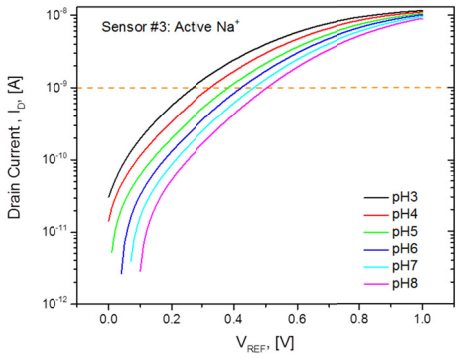

Fig. 14. I_D-V_G characteristics of the sensor#3 (gold gate functionalized for Na^+) for various pH buffers (cross-sensitivity).

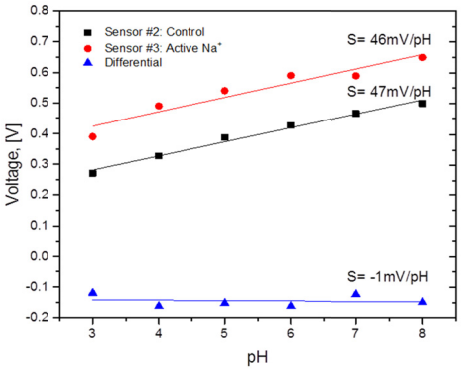

Fig. 15. pH sensitivities of Na^+ functionalized sensor #3 and control sensor #2, proving close-to-zero differential selective sensitivity to pH.

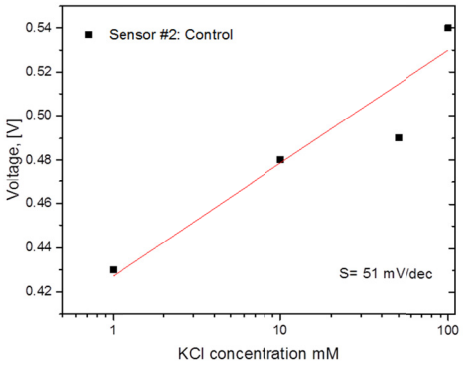

Fig. 16. KCl sensitivity of control sensor #2 (non-functionalized gold gate) needed in differential K^+ differential sensitivity (extracted similarly to Na^+ sensor).

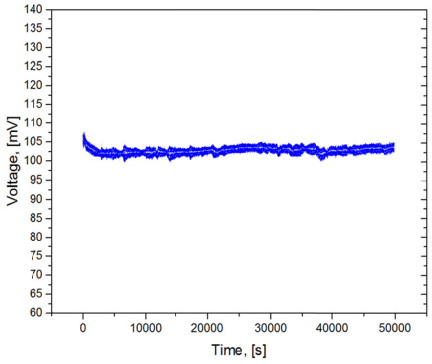

Fig. 17. Stability plot of open circuit potential of the reference microelectrode while perfusing 23 mM NaCl at 25 nl/min through the channel (vs. a commercial flow-through AgCl ref. electrode).